PROCEEDINGS A

royalsocietypublishing.org/journal/rspa

Research

Cite this article: Roy S, Majhi S, Perc M, Ghosh D. 2025 Transitive to cyclic dominance in eco-evolutionary dynamics of strategic species. *Proc. R. Soc. A* **481**: 20240734.
https://doi.org/10.1098/rspa.2024.0734

Received: 27 September 2024
Accepted: 13 December 2024

Subject Category:
Physics

Subject Areas:
complexity, statistical physics

Keywords:
evolutionary game theory, transitive dominance, cyclic dominance, strategic species

Author for correspondence:
Dibakar Ghosh
e-mail: dibakar@isical.ac.in

†These authors contributed equally to the study.

THE ROYAL SOCIETY PUBLISHING

Transitive to cyclic dominance in eco-evolutionary dynamics of strategic species

Sourav Roy[1,†], Soumen Majhi[2,†], Matjaž Perc[3,4,5,6] and Dibakar Ghosh[7]

[1]Department of Mathematics, Jadavpur University, Kolkata, West Bengal, India
[2]Physics Department, University of Rome Tor Vergata, Via della Ricerca Scientifica 1, Rome 00133, Italy
[3]Faculty of Natural Sciences and Mathematics, University of Maribor, Koroška cesta 160, Maribor 2000, Slovenia
[4]Community Healthcare Center Dr. Adolf Drolc Maribor, Ulica talcev 9, Maribor 2000, Slovenia
[5]Complexity Science Hub, Metternichgasse 8, Vienna 1030, Austria
[6]Department of Physics, Kyung Hee University, 26 Kyungheedae-ro, Dongdaemun-gu, Seoul 02447, Republic of Korea
[7]Physics and Applied Mathematics Unit, Indian Statistical Institute, 203 B. T. Road, Kolkata 700108, India

SR, 0009-0004-1744-9792; SM, 0000-0003-0612-6125; MP, 0000-0002-3087-541X; DG, 0000-0003-4832-5210

Eco-evolutionary game dynamics explores the intricate interplay between ecological processes and evolutionary strategies. Here we unveil various transition mechanisms from transitive dominance to cyclic dominance within ecological communities, using evolutionary game theory to model strategic interactions among species. Specifically, we choose a multigame framework that incorporates games that exhibit transitive and cyclic dominance. By integrating appropriate models for transitive dominance and cyclic dominance, and through rigorous numerical simulations and analytical approaches, we explore evolutionary game dynamics under varying conditions. We show that, under specific conditions, communities can change from a linear hierarchy, or transitive dominance, to a cyclical structure, or cyclic dominance, which significantly affects ecosystem community structures. We also show that not only game-independent factors, but also intrinsic game parameters can drive a transition from transitive dominance to cyclic dominance. More precisely, we show how changes in the probability of game selection can lead to this transition. Moreover,

we demonstrate that even benefits arising from free space can facilitate the shift from transitive to cyclic dominance. Our study thus explores the mechanisms that drive transitions between these dominance patterns and, in so doing, we underscore the importance of multiple game dynamics for accurately describing the intricacies of natural ecosystems.

1. Introduction

Ecological and evolutionary changes are closely linked, often occurring simultaneously, with each leaving lasting influence on the other. Eco-evolutionary dynamics [1–3] explains the interplay between such ecological and evolutionary processes. Evolutionary game theory [4–8] explores how strategic interactions between individuals shape the evolution of behaviours in populations, applying population dynamics to game theory [9,10]. The principles of game theory help model strategic interactions among species, providing insight into how these interactions influence community structures. Eco-evolutionary game dynamics offers a powerful framework for understanding the complex interactions between evolutionary strategies and diverse ecological processes, and thus has grown in significance as a field of study. Among the approaches, eco-evolutionary game dynamics subject to strategy-dependent environmental feedback is particularly noteworthy. Wang *et al*. [11] presented an excellent overview of this framework, summarizing the approaches spanning two-player games to multiplayer games, and also highlighting diverse applications of these frameworks across various domains.

Different forms of species dominance, such as genetic, behavioural and ecological, shape eco-evolutionary dynamics by affecting interactions between ecological processes and evolutionary changes [9]. Genetic dominance, where dominant alleles mask recessive ones, influences population evolution by controlling trait visibility. For example, the presence of dominant alleles for pesticide resistance in some insect populations allows rapid adaptation and can lead to population-level shifts in trait distributions. Behavioural dominance, seen in social hierarchies, affects individual fitness and population dynamics by granting dominant individuals better access to resources, which alters reproductive success and survival. For example, dominant wolves and primates secure top resources and mates, driving evolutionary responses related to aggression, cooperation and mate selection. These behavioural dynamics can cause rapid evolutionary responses as individuals adapt to the social structure and competitive environment [1,12].

Ecological dominance can lead to major changes in the community structure, species composition and even biodiversity, which in turn have a noticeable influence on the evolutionary pressures on both dominant and subordinate species. For instance, dominant trees in a forest can alter light and nutrient availability, driving adaptations in shade tolerance or nutrient efficiency in other species [13]. This interplay between ecological dominance and evolutionary adaptation forms feedback loops that drive eco-evolutionary dynamics. These dominance patterns within species and communities shape evolutionary changes and ecosystem stability. Understanding these dynamics is crucial for predicting how species and ecosystems will respond to environmental changes and anthropogenic pressures [14]. Thus, one of the most central concepts in ecological systems is the notion of dominance patterns within ecological communities. For instance, transitive and cyclic dominances are considered to be the two most crucial dominance relationships. Transitive dominance is portrayed by a linear hierarchical relationship where one species consistently outcompetes others (without being outcompeted), forming a clear ranked community structure. On the other hand, cyclic dominance is characterized by a nonlinear, rock-scissors-paper like relationship, where each species outcompetes another, but gets outcompeted by one species, forming a cyclical structure.

Let us dive deeper into the concept of transitive dominance. As mentioned above, transitive dominance refers to a hierarchical structure in which species or individuals dominate others in a linear, rank-based manner, significantly influencing community structure, resource distribution and species interactions. The majority of the earlier research has examined the ecological dominance patterns separately, typically concentrating on either transitive or cyclic dominance within particular ecological settings. For instance, transitive dominance is well documented in various species, including ants, fish, birds and mammals, highlighting its unique dynamics and effects. In tropical forests, the ant species *Azteca trigona* exemplifies transitive dominance by controlling other ants such as *Camponotus sericeiventris* and *Ectatomma ruidum*. This dominance lets *Azteca trigona* monopolize key resources, influencing the distribution and behaviour of subordinate ants [15,16]. In Caribbean coral reefs, *Stegastes planifrons* demonstrates hierarchical dominance over species such as *Stegastes dorsopunicans* and *Microspathodon chrysurus*. Its territorial aggression secures key feeding areas and shelters, affecting the distribution and survival of less dominant damselfish [17]. In primate communities, such as those of *Macaca mulatta* rhesus macaques, well-established hierarchical dominance ensures that dominant individuals receive preferential access to food, mates and resting areas. Subordinates face less favourable conditions, and social behaviours such as grooming, aggression and alliances help maintain order and reduce conflicts [18].

These examples underscore the importance of transitive dominance in shaping ecological interactions and community dynamics. Dominance hierarchies, by influencing resource access and spatial distribution, play a critical role in the survival of species and reproductive success across various ecosystems. In addition, cyclic dominance refers to a fascinating and highly significant dominance pattern observed in several ecosystems. In this phenomenon, species interact in a nonlinear, non-hierarchical way in which each species has an advantage over another in a cyclical arrangement, similarly a rock-scissors-paper game. Cyclic dominance inhibits any single species from gaining excessive dominance and thus facilitates species coexistence and the persistence of biodiversity. This pattern is pertinent in diverse predator–prey interactions, microbial populations and also in plant communities. For instance, this phenomenon is encountered in side-blotched male lizards with different mating strategies, meadow plant communities, coral reef ecosystems, *Escherichia coli* strains, marine molluscs, etc. Owing to its relevance, there exist notable attempts to explore cyclic dominance among different strategies in evolutionary game theory [19,20]. Szolnoki *et al*. [21] expanded traditional pairwise interactions to group interactions in cyclic dominance games, and this shift turned out to influence both the stationary strategy fractions and their dominance relations. Biodiversity in cyclic dominance models is also shown to be maintained through heterogeneity in site-specific invasion rates [22]. In [23], the authors introduced a new path to cyclic dominance in voluntary social dilemmas by adding risk-averse hedgers to the usual cooperators, defectors and loners. Nag Chowdhury *et al*. [24] also observed a novel path to cyclic dominance in which cooperators, punishers and defectors coexist through an inverse Hopf bifurcation, followed by an inverse period-doubling route. In addition, incorporating free space has been shown to stabilize dynamics through cyclic dominance, which arises between the three species: predators, prey and parasites [25].

Despite these studies, research on possible transitions between transitive and cyclic dominance within ecological communities, is barely pursued, and hence the mechanisms underlying such transitions remain particularly unexplored. Our study aims to fill this gap. We, specifically, investigate the ecological and evolutionary conditions driving possible transitions of evolutionary strategies from transitive dominance to cyclic dominance. We formulate a mathematical model integrating games exhibiting both transitive and cyclic dominance patterns within a framework of evolutionary multigame dynamics. This formulation is not only capable of depicting the individual effects of each dominance, but also permits the study of dynamic interplay between these two dominance patterns. Previously, the dynamics of evolutionary multigames has been explored by utilizing prisoner's dilemma and snowdrift games as the

foundation of the model, while incorporating an additional punishment strategy and the ecological concept of free space [26]. Roy *et al*. [27] presented a detailed investigation of eco-evolutionary dynamics of multigames with mutations. On the other hand, from a different perspective, co-evolutionary success-driven multigames in structured populations is studied [28,29]. Evolutionary multigames in structured populations are further explored using the weak prisoner's dilemma [30,31] as the core game, where part of the population adopts either a positive or negative sucker's payoff, engaging in either the traditional prisoner's dilemma or the snowdrift game [32]. Qin *et al*. [33] established that social diversity can enhance cooperation in spatial multigames.

Through rigorous numerical simulations and analytical approaches based on the stability of various equilibria, we reveal that both independent factors of the game and intrinsic game parameters can drive transitions from transitive to cyclic dominance. The probability of game selection drives a transition from transitive to cyclical arrangement of evolutionary strategies. Furthermore, we demonstrate that the availability of benefits arising from free space, often overlooked in traditional models, significantly facilitates the shift from a linear to a cyclical dominance pattern.

2. Model

Our eco-evolutionary multigame framework is based on two fundamental principles of domination of the species: transitive dominance and cyclic dominance. To incorporate these theories into optimality, we first introduce two payoff matrices in our formulation, depicting the cyclic dominance and the transitive dominance, respectively via

$$P = \begin{array}{c} \\ \mathbf{A} \\ \mathbf{B} \\ \mathbf{C} \end{array} \begin{array}{c} \begin{array}{ccc} \mathbf{A} & \mathbf{B} & \mathbf{C} \end{array} \\ \begin{pmatrix} 0 & a & -b \\ -a & 0 & c \\ b & -c & 0 \end{pmatrix} \end{array} \text{ and } Q = \begin{array}{c} \\ \mathbf{A} \\ \mathbf{B} \\ \mathbf{C} \end{array} \begin{array}{c} \begin{array}{ccc} \mathbf{A} & \mathbf{B} & \mathbf{C} \end{array} \\ \begin{pmatrix} 0 & a & b \\ -a & 0 & c \\ -b & -c & 0 \end{pmatrix} \end{array}.$$

where A, B and C are three arbitrarily chosen strategies to portray these two-way dilemmas. The matrix P depicts cyclic dominance, where strategy A wins over strategy B, and strategy B wins over strategy C, but we observe a reversed mannerism while strategies A and C face off. Here, strategy C has a clear win over strategy A with the same magnitude b. The matrix Q, on the other hand, illustrates the transitive domination scenario, where strategy A dominates strategy B with payoff attribute $a \geq 0$. Strategy B also has a strict domination over strategy C by gaining a payoff $c \geq 0$ on the win. The transitivity of strategy A over strategy C is thus seen, where strategy A also receives a clear win over strategy C by gaining the payment amount $b \geq 0$. In our eco-evolutionary framework these two dilemmas are presumed to occur with alternative probabilities in the environment. If p is the probability of shaping the terrain toward cyclic dominance the remaining possibility $(1 - p)$ lets the other scenario of domination conquer the habitat. In summary, we use the probability $p \in [0,1]$ to describe the dilemma which we aim to deliver to depict our interpretation of the eco-evolutionary dynamics of strategic species. Let M be the final version of the payoff matrix, which portrays the ecological terrain's multi-dilemma, taking the following form

$$M = pP + (1-p)Q = \begin{array}{c} \\ \mathbf{A} \\ \mathbf{B} \\ \mathbf{C} \end{array} \begin{array}{c} \begin{array}{ccc} \mathbf{A} & \mathbf{B} & \mathbf{C} \end{array} \\ \begin{pmatrix} 0 & a & b-2pb \\ -a & 0 & c \\ 2pb-b & -c & 0 \end{pmatrix} \end{array}. \tag{2.1}$$

Furthermore, this study adds another key feature by incorporating the concept of ecological free space (F) into the matrix M depicting two dilemmas in alternative possibilities. This altruistic

characteristic of the ecological free space providing benefits to replicate enlarges the 3 × 3 payoff matrix M, into a 4 × 4 matrix as

$$M = \begin{array}{c} \\ \mathbf{A} \\ \mathbf{B} \\ \mathbf{C} \\ \mathbf{F} \end{array} \begin{array}{c} \begin{array}{cccc} \mathbf{A} & \mathbf{B} & \mathbf{C} & \mathbf{F} \end{array} \\ \begin{pmatrix} 0 & a & b-2pb & \sigma_A \\ -a & 0 & c & \sigma_B \\ 2pb-b & -c & 0 & \sigma_C \\ 0 & 0 & 0 & 0 \end{pmatrix} \end{array}. \tag{2.2}$$

Here, σ_A, σ_B and σ_C are the positive attributes contributed by the ecological free space (F), which support the replication of species adopting strategies A, B and C, respectively. To deduce the average fitness of the species, we consider both the abundance of the species and the abundance of free space, as described by the payoff matrix (2.2), within a unit size terrain.

Let x, y and z represent the abundances of species adopting strategies A, B and C, respectively, and let w denote the frequency of ecological free space (F). Given that the total abundance must sum to one, we have the constraint $x + y + z + w = 1$. When calculating the average fitness of the species, we employ the additional constraint $w = 1 - x - y - z$. Thus, the average fitness f_i for species i (where i corresponds to strategies A, B or C) can be expressed as

$$\begin{aligned} f_A &= ay + (b-2pb)z + \sigma_A w = -\sigma_A x + (a-\sigma_A)y + (b-2pb-\sigma_A)z, \\ f_B &= -ax + cz + \sigma_B w = -(a+\sigma_B)x - \sigma_B y + (c-\sigma_B)z, \\ f_C &= (2pb-b)x - cy + \sigma_C w = (2pb-b-\sigma_C)x - (c+\sigma_C)y - \sigma_C z, \end{aligned} \tag{2.3}$$

where f_A, f_B and f_C provide a comprehensive representation of the average fitness of each species, considering the contributions from both inter-species interactions and the ecological free space. Now, considering three positive rates of extinction α, β and γ for three different abilities A, B and C; we deduce the eco-evolutionary dynamical form of this multi-dilemma model as $\frac{d(\text{abundance})}{dt} = \text{abundance}(\text{birth rates} - \text{death rates})$, reaching our final version as

$$\begin{aligned} \dot{x} &= x(f_A - \alpha) = x(-\sigma_A x + (a-\sigma_A)y + (b-2pb-\sigma_A)z + (\sigma_A - \alpha)), \\ \dot{y} &= y(f_B - \beta) = y(-(a+\sigma_B)x - \sigma_B y + (c-\sigma_B)z + (\sigma_B - \beta)), \\ \dot{z} &= z(f_C - \gamma) = z((2pb-b-\sigma_C)x - (c+\sigma_C)y - \sigma_C z + (\sigma_C - \gamma)), \\ \dot{z} &= -\dot{x} - \dot{y} - \dot{z}. \end{aligned} \tag{2.4}$$

We aim to conduct several numerical experiments with this model (equation (2.4)) to observe how strategic traits change in response to various parameters of the system. For this, we utilize the Runge–Kutta-45 method to solve this set of differential equation (equation (2.4)).

3. Results

Our proposed eco-evolutionary system, as described by equation (2.4), reveals multiple modes of interaction among various species within the considered environment, depending on the parameter values explored. Specifically, the parameters a, b and c (all positive) emphasize the payoff weights of the player species during their corresponding strategic interactions through these two dilemmas. On the other hand, the parameters σ_A, σ_B and σ_C (also positive) represent additional replicatory factors that arise from the altruistic kind of ecological free space (F). The parameter p, ranging from 0 to 1, determines the likelihood of cyclically dominant strategies among the species from the hierarchical influence of the first strategy on the other two, aligned with the findings of Roy *et al*. [34]. Such frameworks are essential for understanding the dynamics of species interaction and evolution within ecological networks, and their applications can be seen in studies of cooperative behaviour in structured populations [35], as well as in cyclic competition models in which species participate in rock-paper-scissors dynamics

[19]. In the following, we sequentially investigate the consequences of varying the system parameters, emphasizing how different probabilities p lead to a range of novel outcomes.

(a) Consequences of cyclic dominance for $p = 1$

Before exploring the uncharted literature on eco-evolutionary dynamics in transitive dominance among species' strategies, and the gradual shift in interaction modes from transitive to breaking into cyclic patterns, we first discuss some basic features regarding the abundance of fully cyclically dominating traits, assuming the probability $p = 1$. The payoff matrix P describes a fully cyclic payoff matrix and delivers its attributes a, b and c describing the inter-strategic interactions among strategies A, B and C. This cyclic pattern between the payoffs depicts a similar portrayal as the rock-scissor-paper dilemma game [34]. As previously studied works encapsulate this mechanism of cyclical dominance in both ecology and evolution [19,36–39], in this study, we execute two experiments that show the cyclic spectrum in the abundance of strategic species (see figure 1). With the preliminary setting of $p = 1$, we fix the other parameters at $a = 1, b = 1.5, c = 1.2, \sigma_A = 1.5, \sigma_B = 1.7, \sigma_C = 1.25, \alpha = 0.15, \beta = 0.4$ and $\gamma = 0.25$. In this setting, the cyclic eco-evolutionary system develops into an oscillatory spectrum, where over time, each strategy cyclically occupies the ecological terrain by defeating the corresponding weaker one, as observed in the time series frequency of the strategic species (figure 1*a*). Eventually, the three-dimensional phase portrait diagram endorses a fully closed trajectory corresponding to the stable oscillation of these traits (see figure 1*b*). Another interesting rhythm of oscillation is seen from the parameter set $a = 0.25, b = 0.4, c = 0.55, \sigma_A = 0.52, \sigma_B = 0.60, \sigma_C = 0.72, \alpha = 0.10, \beta = 0.2, \gamma = 0.24$ and $p = 1$. In the setting, our system (equation (2.4)) yields three pseudo-stable equilibrium points, specifically, $A_1(0.8077, 0, 0)$, $A_2(0, 0.667, 0)$ and $A_3(0,0,0.667)$, each one promotes the supremacy of the three proposed strategies A, B and C, respectively. However, owing to their instability and the cyclic tendency to be defeated by the preceding strategy, each equilibrium fails to maintain the solo dominance of any of these proposed strategies, instead breaking into consecutive plateau-like regimes that mirror the cyclic oscillations of x, y and z (figure 1*c*). Similarly, the three-dimensional portrait of these strategic species unveils a triangular-shaped closed trajectory, with each vertex corresponding to one of the three equilibria: $A_1(0.8077, 0, 0)$, $A_2(0, 0.667, 0)$ and $A_3(0,0,0.667)$ (see figure 1*d*).

The next part of our study focuses on examining on the whole span of how the cyclic-modified payoffs captivate the framework starting from the hierarchical dominance.

(b) Transition from transitive dominance to cyclic dominance

One of the most intriguing and important scenarios we focus on in our study is the continuously evolving trajectory in the abundance of the strategic species with the increasing probability p, and how the mode of domination gradually shifts from transitive to cyclic with this increasing factor. For the experiment, we fix the set of parameters at $a = 1, b = 1.5, c = 1.2, \sigma_A = 1.5, \sigma_B = 1.7, \sigma_C = 1.25, \alpha = 0.15, \beta = 0.45$ and $\gamma = 0.25$, and vary the probability $p \in [0,1]$ taking a step length of 0.01. At and after $p = 0$, the domination is solely led by the strategy A and its associated species, exhibiting a stable and constant abundance of 90% ($A_1(0.9, 0, 0)$) up to $p = 0.54$ (grey background in figure 2*a*,*e* unveils the time series taking probability $p = 0.5$). After overcoming a long possible way, the stable and hierarchical method of domination by the single strategy A over the other two breaks onwards $p = 0.54$. This is because the possibility for strategy A to dominate strategy C gradually decays with growing p, affecting the corresponding payoff value in the matrix M. Thus, the C-strategic species show a noticeable jump with the increase in possibility p from 0.54 to 0.55. Subsequently, the growing feature in the species allows a small possible region to rise, approximately $p = 0.55$,

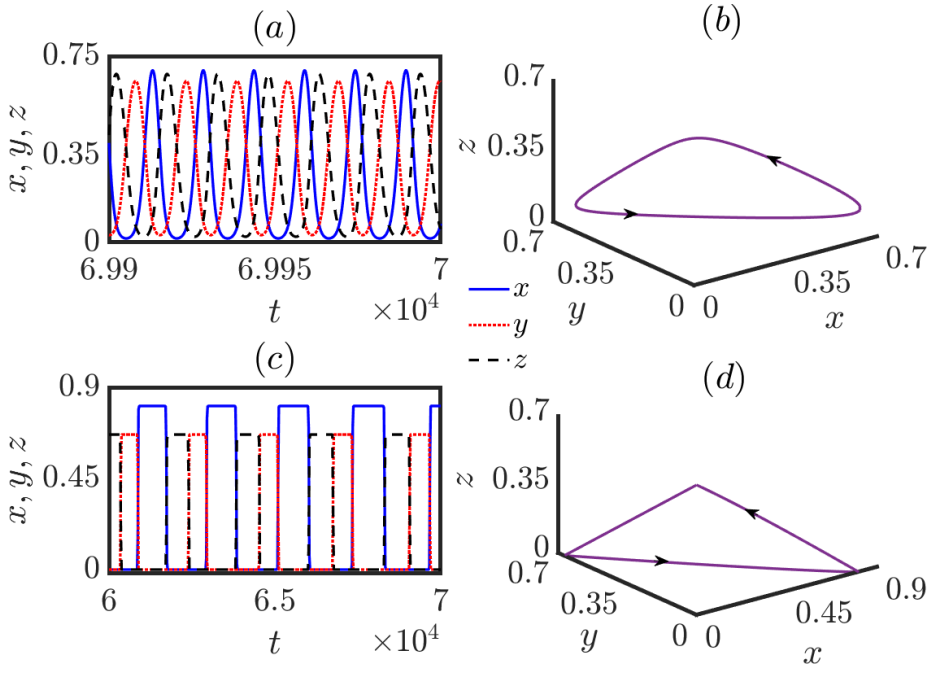

Figure 1. Oscillatory features of cyclic domination among strategies and their kind species: this figure captivates the cyclic oscillations and three-dimensional phase portrait captured by the fully cyclic payoff matrix by setting $p = 1$ and setting other parameters at $a = 1, b = 1.5, c = 1.2, \sigma_A = 1.5, \sigma_B = 1.7, \sigma_C = 1.25, \alpha = 0.15, \beta = 0.4$ and $\gamma = 0.25$ (time series captured in (*a*), while the phase portrait diagram is presented in (*b*)); and $a = 0.25, b = 0.4, c = 0.55, \sigma_A = 0.52, \sigma_B = 0.60, \sigma_C = 0.72, \alpha = 0.10, \beta = 0.2$ and $\gamma = 0.24$ ((*c*) and (*d*)). We take the same initial abundance for each strategic trait (0.3,0.3,0.3). We primarily observe two distinct types of oscillations yielding fully cyclic strategies, as indicated by the time series. The second type, pseudo-stable oscillation, allows each strategy to transiently dominate the system, maintaining a dynamic equilibrium where no single trait achieves permanent dominance, thereby facilitating temporal coexistence.

where particularly two strategies A and C, and their kind species get a chance to survive having reciprocal abundances to each other (cyan region in figure 2*e*, and represented by time series (*b*) at $p = 0.55$, describing one of the planar equilibrium points $A_6(x^*, 0, z^*)$). Furthermore, with the growth in the abundance of the C species, the chances of survival of strategy B also increase. Thus, at and after $p = 0.56$, we witness that the three proposed strategic species (A, B and C) coexist and sustain themselves together. Moreover, we observe an increasing frequency of the B-strategic species along with the parallel decaying flows in the abundance of both A- and C-strategic species up to $p = 0.84$ (see the time series at figure 2*c*, and brown region describing the coexisting stationary point $A_7(x^*, y^*, z^*)$ in figure 2*e*). The structure of eco-evolutionary dynamics changes its shape of stability after 84% probability of species exhibiting cyclic behaviour. This leads to a breakdown of the previously stable coexistence of species, transitioning into oscillatory behaviour through a super-critical Hopf bifurcation occurring at $p = 0.84$, and continuing until the payoff structure of the strategies becomes fully cyclic at $p = 1$ (unstable region marked by the yellow background in figure 2*e*, and the oscillatory time series evolution is represented by figure 2*d*).

(c) The interplay of different system parameters on the varying span of p

After addressing the variation in the abundance of strategic traits in relation to the probability p in the considered range [0,1], we centralize our motive on the underlying effects of

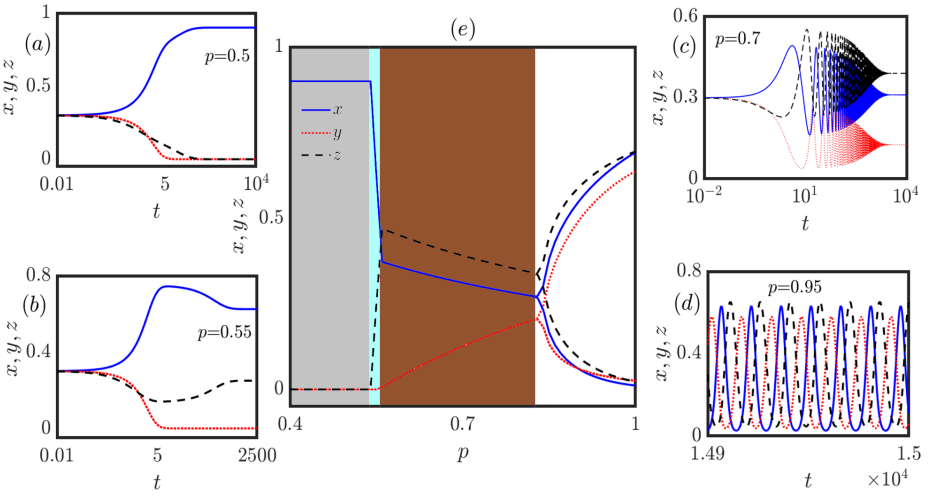

Figure 2. The fluctuation of probability p within the range [0.4,1] governs the shift from transitive species dominance to cyclic dominance: The large central diagram represents the bifurcation diagram of our system (equation (2.4)) for the probability factor p from 0.4 to 1. Our motive is to captivate the variation of p from 0, but as the phenomenon remains the same for $p = 0$ to $p = 0.54$, we omit the portion up to $p = 0.4$. Three consecutive steady states, A_1, A_6 and A_7 appear while varying p from 0.4 up to 0.84 represented by grey, cyan and brown backgrounds, respectively. Onwards, a cyclically dominating oscillatory pattern starts appearing and persisting up to $p = 1$, the full possible regime for the payoffs to become cyclic.

altering the other system parameters along with the probability p of changing the nature of the payoff interactions. For this, we make three consecutive experiments using three different factors, that is, one payoff attribute b, one additional free space induced benefit σ_B towards the B-strategy kinds and one linear extinction rate factor α, denoting the mortality rate of the A-strategic species that can notably influence the dynamical consequences of our system (equation (2.4)). We moreover fix all our system parameter values at $a = 0.6, b = 0.1, c = 0.4, \sigma_A = 0.75, \sigma_B = 0.8, \sigma_C = 0.9, \alpha = 0.35, \beta = 0.2$ and $\gamma = 0.08$ for each experiment depicted in figure 3 other than the experimented parameters.

The first experiment is based on one of the concerned payoffs b in the range (0,2], considered effective when the interaction between A and C-strategic species is fully reversed in relation to these strategies at $p = 0$ and $p = 1$. With the increasing possibility of taking the shape of a completely cyclic payoff structure in terms of increasing p, the C-strategic species obtains a fair chance to compete for evolution as the payoff b ensures their gain. Thus with a fairly high possibility from $p = 0.4$ up to $p = 1$, we observe the coexistence of all three strategies and their associated species, allowing them to survive together (brown region in figure 3*a*). However, three consecutive scenarios appear when we continuously increase the value of b in the highly transitive regime of the payoff kinds. At the fully transitive payoff zone ($p = 0$), and while b receives a low frequency, the chance of strategy A to dominate strategy C remains very low, thus the coexistence continues to remain steady up to $b = 0.38$. Once that point is crossed, strategy A's domination ability strengthens, establishing a hierarchical order of dominance. The B strategies are observed to be eliminated first (see the cyan region representing state $A_6(x^*, 0, z^*)$), and the coexistence of only two strategic species A and C is observed for some frequencies of b. Nevertheless, once $b = 0.64$ is surpassed, the possibility of eliminating the C-strategic species increases in favour of the A species. Eventually, for the remaining values of b, only the A-strategic species solely dominate the habitat (grey region in figure 3 denotes the state $A_1(x^*, 0, 0)$), and with the increasing p, the thresholds of payoff b also rise for the emergence of these two states compared with the state of coexistence.

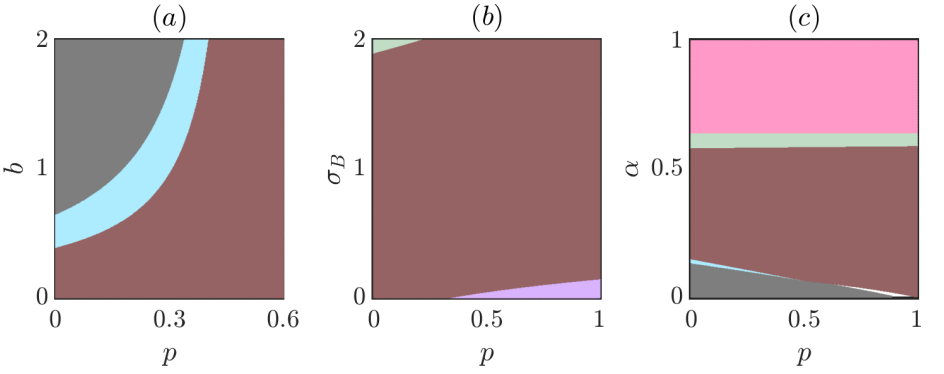

Figure 3. Parameter space concerning the increasing p, the probability for the transformation of transitive payoff to become fully cyclic over three other parameters b, σ_B and α: this figure diagram captures the two-dimensional spans concerning p with b (*a*), σ_B (*b*) and α (*c*). For all these experiments, we fix our initial frequency at (0.3,0.3,0.3) and observe the dynamics above 50 000 times up to 60 000 time iterations. We take step length $h = 0.01$ for each parameter used for the experiments. In these diagrams, various forms of steady attractors and unstable zones emerge, as detailed in the main text. To enhance clarity, we represent the steady states with distinct colours, visually highlighting their stability and distinguishing them from regions of instability.

However, the variation of the factor $\sigma_B \in (0,2]$ related to the free-space induced benefit, with respect to $p \in [0,1]$ yields three stable regimes. As σ_B serves directly to the strategy B; the high frequency of σ_B affects the B-strategic traits positively. Thus the high abundance of strategy B is driven by the gradual increase of σ_B and the consistent influence of strategy A collectively exerts a significant effect on the survival of strategy C and its species within the elevated transitive regime. So, for $p \leq 0.21$, we find a small portion linearly decreasing with the rising probability p, where only the A and B strategic species can coexist sustainably (olive-green region in figure 3 denoting $A_4(x^*, y^*, 0)$). On the other hand, when the probability of the payoff structure becoming cyclic increases, starting from $p = 0.33$, a small range emerges where the A-strategic species cannot coexist with the other two species (purple portion in figure 3*b* defining the stable state $A_5(0, y^*, z^*)$). This A strategy-free stable planar state occurs only at very low frequencies of σ_B, even though a lower amount of σ_B generally reduces the prospect for the B species to sustain. For the fully cyclic structure of the payoff attributes, i.e. at $p = 1$, this dual strategic stability holds for $\sigma_B = 0.14$. Apart from these, the stable coexistence of three strategies and their kind species is found for the rest of the two-dimensional space (brown region in figure 3*b*).

The experiment investigating the variation in the extinction frequency of A-strategic traits α within the range (0,1], along with the probability factor p, reveals diverse patterns of strategic stability among these species (see figure 3*c*). As the likelihood of A-strategy extinction rises, strategy A is ultimately driven to extinction, leading to a region beyond $\alpha = 0.63$ where neither A- nor C-strategic species can survive, regardless of the probability p (pink region, $A_2(0, y^*, 0)$). Between $\alpha = 0.58$ and 0.63, there is a region where both A and B species coexist (olive-green region, $A_4(x^*, y^*, 0)$), and a larger region exists where all three strategic species coexist (brown region, $A_7(x^*, y^*, z^*)$). As p increases, a shrinking region emerges where A-strategic species exclusively dominate the habitat (grey region, $A_1(x^*, 0, 0)$). As the likelihood of cyclical payoff structure rises, the dominance of strategy A diminishes and eventually disappears at $p = 1$. In addition, a narrow unmarked area in figure 3*c* indicates that the stable existence of all the strategic species breaks down into an oscillatory regime when a high probability p is introduced. At lower p values, a narrow region appears where only A and C species can survive (cyan region, $A_6(x^*, 0, y^*)$). However, as p increases, this regime also loses stability and transitions into a coexistence of all the strategic species takes place.

4. Characteristics of transitive dominance for $p = 0$

The central focus of our study explores the characteristics of the hierarchical and non-cyclic payoff structure of the strategic attributes A, B and C. The considered structure of the payoff matrix Q (at $p = 0$ of matrix (2.2)), indicates a clear domination over strategy C from both sides of strategy A and B together. Moreover, strategy B is also seen to be conquered by strategy A. *For the first time,* we explore the eco-evolutionary dynamics of this game-theoretic structure, where A-strategic species invade B-strategic species with a positive payoff a, and B-strategic species, dominate C-strategic species with payoff c. Further, A-strategic species, in turn, invade C-strategic species yielding a positive payoff b. Taking this scenario in our account, our system (equation (2.4)) becomes

$$\begin{aligned}\dot{x} &= x[-\sigma_A x + (a-\sigma_A)y + (b-\sigma_A)z + (\sigma_A - \alpha)],\\ \dot{y} &= y[-(a+\sigma_B)x - \sigma_B y + (c-\sigma_B)z + (\sigma_B - \beta)],\\ \dot{z} &= z[-(b+\sigma_A)x - (c+\sigma_C)y - \sigma_C z + (\sigma_C - \gamma)].\end{aligned} \tag{4.1}$$

Unlike a cyclic takeover, strategy A consistently outperforms both B and C, with a decisive victory over strategy C marked by the positive payoff b. Although the salient point about the interplay of strategies generalizes the concept that, over time, only strategy A achieves full dominance over the others, our mathematical framework (equation (4.1)) roots around several factors in it, including the free space provided benefits σ_A, σ_B and σ_C, and the linear factors such as α, β and γ, depicting their rates towards extinction. Owing to the inclusion of various factors affecting the basic payoffs of the species, the model (equation (2.4)) yields several stationary or equilibrium states for $p = 0$.

At $a = 1, b = 1.5, c = 1.2, \sigma_A = 1.5, \sigma_B = 1.7, \sigma_C = 1.25, \alpha = 0.15, \beta = 0.45$ and $\gamma = 0.25$, as per the previous section, we obtain a clear win of strategy A, surviving its kind species at a constant abundance of 0.9, with all other strategic traits going to an extinction (see figure 4*a*). This set of parameters provides a clear view of the key feature revealed through the transitive dominance of species. Mathematically, this stable solo-strategic environment depicts one of the axial attractors $A_1(x^*, 0, 0)$ of our proposed system (equation (2.4)), where the A-strategic species (0.9,0,0) can only survive in the race of evolution. Keeping the payoff amounts a, b and c to be the same, we intend to tune other parameters and set them to $\sigma_A = 0.8, \sigma_B = 1.7, \sigma_C = 0.8, \alpha = 0.5, \beta = 0.4$ and $\gamma = 0.35$. We witness another significant equilibrium state of our system as $A_4(x^*, y^*, 0)$, where $x^* = 0.4053$, and $y^* = 0.1211 (< x^*)$, as in figure 4*b*. This stable state endorses the stable coexistence of only two strategies, keeping their kind species' abundances in hierarchical order ($x^* > y^*$). This stratified order can be altered with the tuning of three of these parameters. We fix $\sigma_A = 0.5, \sigma_B = 0.25$ and $\gamma = 0.2$, keeping all other factors fixed as the previous state. Surprisingly, the weak C strategy is strengthened by ensuring that C-strategic species can survive alongside A-strategic species with an abundance of 0.111, and we also witness a downfall in the abundance of A-strategic species (0.222). Figure 4*c* portrays the stability of the planar equilibrium $A_6(x^*, 0, z^*)$ in the absence of B-strategic species in the habitat.

An interesting situation arises while we fix our parameter values at $a = 0.6, b = 0.1, c = 0.4, \sigma_A = 0.75, \sigma_B = 0.8, \sigma_C = 0.9, \alpha = 0.35, \beta = 0.2$ and $\gamma = 0.08$. With this set of parameter values, the proposed system supports the survival of all the proposed strategies and their respective species (see figure 4*b*) in a notable sequence. Despite minimal differences among the free space attributes to the species, and only slight variations in the payoff attributes a, b and c, the abundance of the weakest strategy C generally exhibits the highest abundance of 0.3404. Following that, the B strategy owns an abundance of 0.2503, and noticeably, the strategy A (that generally keeps the strongest hold in the transitive dominance framework) here exhibits the lowest frequency of 0.1883, thus resulting in the stabilization of the attractor ($A_7(0.1883, 0.2503, 0.3404)$). The 'survival of the weakest' mechanism plays a crucial role in preserving biodiversity by preventing any single strategy from dominating as the strongest

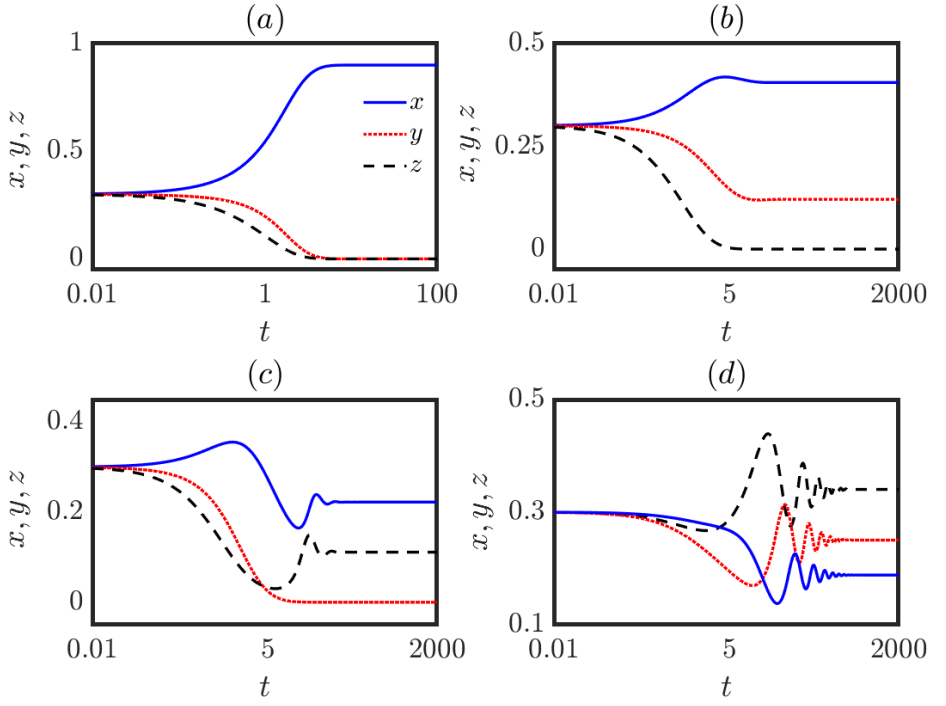

Figure 4. Different strategic states appeared from the transitive dominance of the strategic species: these four time series diagrams verify different stable strategic equilibriums formed by our model (equation 2.2) at $p = 0$. (*a–d*) represent the states $A_1(x^*, 0, 0)$, $A_4(x^*, y^*, 0)$, $A_6(x^*, 0, z^*)$ and $A_7(x^*, y^*, z^*)$, respectively. Although the transitive dominance by strategy A, and its kind species (x) hold utmost supremacy in the general scenario, we verify other strategic species can also make a stable rise in their abundance over A, though we take (0.3,0.3,0.3) as each experiment's initial frequency of the three proposed strategic traits. In the sub-figure (*d*), an unusual behaviour appears, as the abundance of C-strategic species remains the highest whereas, the A-strategic species maintain the lowest abundance.

one. In ecosystems where weaker competitors are not entirely driven to extinction, they can counterbalance the population of stronger species through cyclic or feedback dynamics. The dynamic nature of our system (equation (2.4)) prevents strategy A from monopolizing resources, thereby allowing a greater variety of species to coexist. By sustaining these weaker species, ecosystems maintain a diverse range of traits and interactions, which enhances resilience and stability in the face of any environmental changes. All the experiments have been executed by initiating the frequency of each strategic trait with the same magnitude (0.3,0.3,0.3).

(a) Bifurcations with respect to individual parameters

After presenting potential outcomes within the transitive payoff framework, we now adjust additional system parameters of our system (equation (2.4)) to examine how stable strategic states develop as the frequency of strategic species shifts monotonically in response to these changes. This experiment has been carried out across three different cases, capturing the transition from fully transitive to fully cyclic structured payoffs, i.e. $p \in [0,1]$. More specifically, we tune three distinct parameters in desired ranges taking a step length of 0.01 for each setting of three fixed probabilities p, namely, $p = 0$ (see figure 5*a–c*), $p = 0.5$ (see figure 5*d–f*) and $p = 1$ (see figure 5*g–i*), and fix other parameters at $a = 0.6$, $b = 0.1$, $c = 0.4$, $\sigma_A = 0.75$, $\sigma_B = 0.8$, $\sigma_C = 0.9$, $\alpha = 0.35$, $\beta = 0.2$ and $\gamma = 0.08$, apart from the one we vary.

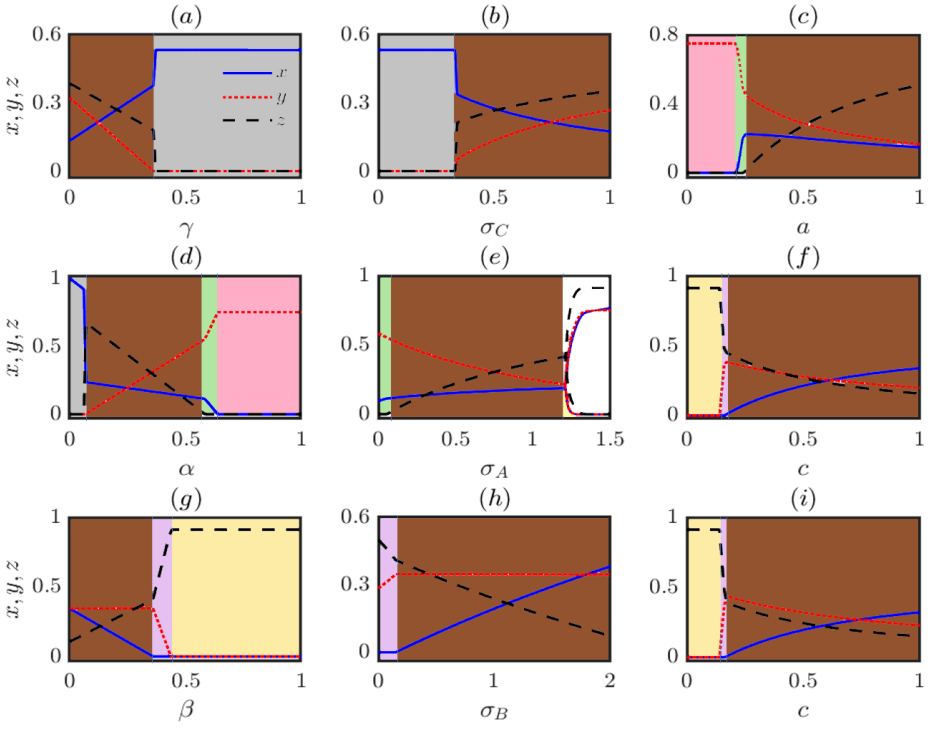

Figure 5. Consequences of single parameter bifurcation for $p = 0, 0.5$ and 1: This figure diagram portrays the variation of the strategic species and their stability concerned to different induced parameters at three different payoff structures. Sub-figures (*a–c*) illustrate the dynamics under a fully transitive payoff structure, while sub-figures (*d–f*) depict the system's behaviour with a semi-transitive, semi-cyclic payoff configuration. The remaining diagrams (*g–i*) represent a fully cyclic payoff structure. Our objective is to investigate the impact of varying system parameters, and thus, each experiment involves variations of different parameters to assess their influence on the observed dynamics. We take the same initial abundance of the strategic species for these numerical simulations, specifically, (0.3,0.3,0.3), and take 700 000 time iterations among which we deduct 600 000 initial iterations as transcend. The background colours represent stable strategic regimes as said in the main text to mark the span of the used parameter in each experiment.

For a fully transitive evolutionary environment, i.e. for $p = 0$, we first vary the rate of extinction of C-strategic species γ in the range (0,1], yielding two consecutive stable strategic states with an interesting trajectory in the abundance of the traits. For a large regime, up to $\gamma = 0.36$, three proposed strategies coexist in the habitat, with the C species showing an obvious decline owing to the increasing γ. As the C species decreases, the B-strategic species, overpowering strategy C also gradually diminishes. In addition, the A-strategic species steadily increase, benefiting from the dual defeats of both C and B strategies in this regime (brown portion pointing the stable coexistence $A_7(x^*, y^*, z^*)$ in figure 5*a*). At $\gamma = 0.37$, the B species experiences a continuous decline, preventing it from sustaining its population, and eventually leading to its extinction. The elimination of strategy B triggers the extinction of C-strategic species, resulting in a sudden fluctuation in their population levels. Interestingly, a sudden jump is also noticed in the frequency of the A species, making them the only surviving strategy holding a constant frequency of 0.53 in the eco-evolutionary habitat onwards up to $\gamma = 1$ ($A_1(x^*, 0, 0)$ indicated by the grey region in figure 5*a*). The varying span of σ_C in (0,1], providing direct benefit to the C-strategy, on the other hand, contributes an exact opposite consequence in the appearance of the strategic state from the previously conducted experiment (see figure 5*b*). Up to $\sigma_C = 0.33$, a constant dominance of the hierarchically fittest strategy A with a continual abundance 0.54 is observed (grey regime describes $A_7(x^*, 0, 0)$ in figure 5*b*). As the ecological contribution of free space increases, there is a sudden rise in the frequency of strategy C holders, which

also provides a fair chance for the B-strategic species to increase. Thus, from $\sigma_C = 0.34$, the coexistence of three strategies is observed (brown range describes $A_7(x^*, y^*, z^*)$ in figure 5*b*). Surprisingly, at $p = 0$, the range of the payoff a allows the B-strategic species to compete effectively for evolutionary dominance up to $a = 0.21$, resulting in a consistent abundance of 0.75. Beyond that point, the B-species begins to experience significant losses, as the payoff a increasingly favours strategy A over strategy B. Eventually, the A-strategic species begins to increase, creating a narrow range of a where only A and B species coexist with reciprocal changes in their abundances (green region in figure 5*c* describes $A_4(x^*, y^*, 0)$). Interestingly, with the rise of strategy A, strategy C starts to gain prominence from $a = 0.25$. The increasing abundance of the C-strategic species exceeds the frequencies of both A and B strategies. This coexistence of all three strategic species extends across the entire range of a up to 1 (brown region in figure 5*c*).

(i) Single parameter bifurcations tune the semi-transitive payoff structure at $p = 0.5$

At $p = 0.5$, the payoff values represent a semi-transitive form, managed by the proposed strategies A, B and C. The semi-transitive structured payoff matrix, using the specified parameter values, takes the following shape:

$$M_{p=0.5} = \begin{array}{c} \\ \mathbf{A} \\ \mathbf{B} \\ \mathbf{C} \\ \mathbf{F} \end{array} \begin{array}{c} \begin{array}{cccc} \mathbf{A} & \mathbf{B} & \mathbf{C} & \mathbf{F} \end{array} \\ \begin{pmatrix} 0 & 0.6 & 0 & 0.75 \\ -0.6 & 0 & 0.4 & 0.8 \\ 0 & -0.4 & 0 & 0.9 \\ 0 & 0 & 0 & 0 \end{pmatrix} \end{array}.$$

This structure reveals a reduced level of challenge for strategy C in terms of its attributes. We thus aim to tune the extinction rate of the A-species α first, which leads to the emergence of the dominant rule of the A-species with a steadily decreasing abundance until $\alpha = 0.6$ (grey portion in figure 5*d*). However, as α increases further, the weaker side of strategy A is revealed, as both strategies B and C rise (brown span indicates the regime of coexistence in figure 5*d*). Another interesting observation is that the C-strategic species experience a rapid increase in abundance alongside the rise of the B species. However, C remains weak against both A and B species, leading to a declining trend in its population. Ultimately, the C species cannot sustain itself beyond the threshold of $\alpha = 0.58$. Beyond this point, the stable coexistence collapses, leaving only the A and B species to survive, with their frequencies fluctuating in a reciprocal manner (green span in figure 5*d*). As the mortality rate of the A-species increases steadily, they eventually become extinct at $\alpha = 0.64$. From $\alpha = 0.64$ to $\alpha = 1$, stability is maintained solely by the B-strategic species, consistently dominating with a fixed abundance of 0.75 (pink portion in figure 5*d*). The variation of σ_A in [0,1.5], providing direct evolutionary welfare to the A kinds yields a small portion up to $\sigma_A = 0.05$, where both A and B strategic species coexist (green span in figure 5*e*). The free space-driven attribute σ_A providing direct benefit to ability A, also causes the weakest strategy C an opportunity to enhance its kind species, and from $\alpha = 0.06$, a stable coexistence of these three strategic species is observed (brown portion in figure 5*e*). On reaching $\sigma_A = 1.21$, the stable coexistence breaks into cyclic oscillation through a super-critical Hopf bifurcation. Thereafter, the stable nodes break into two branches, representing the maximum and minimum abundances in the oscillatory dynamics (unmarked portion in figure 5*e*). Interestingly, a significant range where the weakest strategy C dominates at a constant frequency of $z^* = 0.912$ is observed, for the variation of the payoff c (cream coloured span in figure 5*f* describes $A_3(0,0,z^*)$) up to $c = 0.14$. Subsequently, as c exceeds 0.14, the B-strategic species begin to dominate, along with a strategy, though only over a very narrow range (purple span depicting $A_5(0, y^*, z^*)$ in figure 5*f*). As strategies B and C rise together, the superior strategy A emerges. With a steady increase in its abundance, the A-species eventually surpasses both B

and C species. This leads to a stable coexistence of all three strategic species across the range up to $c = 1$ (brown span, the stable coexisting state $A_7(x^*, y^*, z^*)$ in figure 5*f*).

(ii) Single parameter bifurcations for cyclic chain in payoffs at $p = 1$

At $p = 1$, a fully cyclic payoff structure among the strategies leads to the emergence of several strategically stable states within our system (equation (2.4)). As we vary β, the extinction rate for the B-strategic species spans a wide range, up to $\beta = 0.35$, at which point all three proposed strategies coexist and collectively dominate the environment (brown portion in figure 5*g*). Interestingly, as the likelihood of eliminating the B-species increases, a more rapid decline is observed in the A species compared with the B species. This gradual decline benefits the C species, allowing it to expand its population. After $\beta = 0.35$, A-strategic species are unable to survive and compete in the habitat. This leads to a range, extending up to $\beta = 0.43$, where the B and C strategies form a stable coexistence, while reciprocally swirling (purple portion in figure 5*g*). As the extinction rate rises, the B species continue to decline, and as β approaches 1, a significant range of β emerges where the strategy C dominates exclusively with a constant frequency of $z^* = 0.912$ (cream coloured region in figure 5*g*). The increasing σ_B, which represents the benefit to enhance the welfare of the B species, results in the emergence of two strategically stable zones. Up to $\sigma_B = 0.15$, no presence of the A species is observed, with only the B and C species remaining in the system (purple zone describes the stable $A_5(0, y^*, z^*)$ in figure 5*h*). In this regime, we observe a slight increase in the abundance of the B species, while the C species experience a decline. Subsequently, as the A-strategic species start to emerge, the remaining range of σ_B up to two supports the stable coexistence of all three strategies—A, B and C—along with their respective species in the habitat (brown portion in figure 5*h*). In this stable co-existence, a notable gradual increase in the A-strategic species is observed, whereas the contribution of strategy B does not grow significantly. Ultimately, the frequency of the A species surpasses that of all other strategies. By contrast, the frequency of the B species remains nearly constant or slightly decreases as σ_B increases. The variation of the payoff c (figure 5*i*) remains almost the same as the experiment conducted for $p = 0.5$ (figure 5*f*). The interested reader can check the consequences of varying c for that experiment to understand and analyse the variation of c at $p = 1$.

(b) Two-dimensional parameter space analysis

One of the noble features that unfolds through our study of eco-evolutionary model (equation (2.4)), is that by adjusting certain system parameters within their considered range, we witness a transition from a transitive payoff structure to a fully cyclic one. This tuning reveals how the hierarchical dominance of strategy A diminishes and exposes various stable (or unstable) patterns shaped by the strategic species. For all these experiments, we set the payoff mode according to the matrix Q by keeping $p = 0$, and set our parameter values as $a = 1, b = 1.5, c = 1.2, \sigma_A = 0.5, \sigma_B = 0.25, \sigma_C = 0.80, \alpha = 0.5, \beta = 0.4, \gamma = 0.2$ except for the two varying ones for each experiment as described by figure 6.

First, we examine the distribution of stable strategies across different ranges of the two consecutive payoff attributes b and c, through figure 6*a*. Within their spans, four distinct stable strategic states emerge. Initially, with moderate increments in both payoffs, a square-shaped region appears, bounded by $b = 0.5$ and $c = 0.45$, where only the C-strategic species survive, overpowering all others despite a high value of $a = 1$, which would typically favour the sustainability of strategy A (this is shown by the cream region, representing the state $A_3(0,0,z^*)$). As b increases beyond 0.5, our transitive eco-evolutionary model shifts, allowing strategy A to shift to benefit its own kind in conjunction with strategy C. The increased b enhances the hierarchical strength of strategy A, enabling it to coexist with C (cyan region, representing $A_6(x^*, 0, z^*)$). Conversely, a higher value of c above 0.45 provides similar

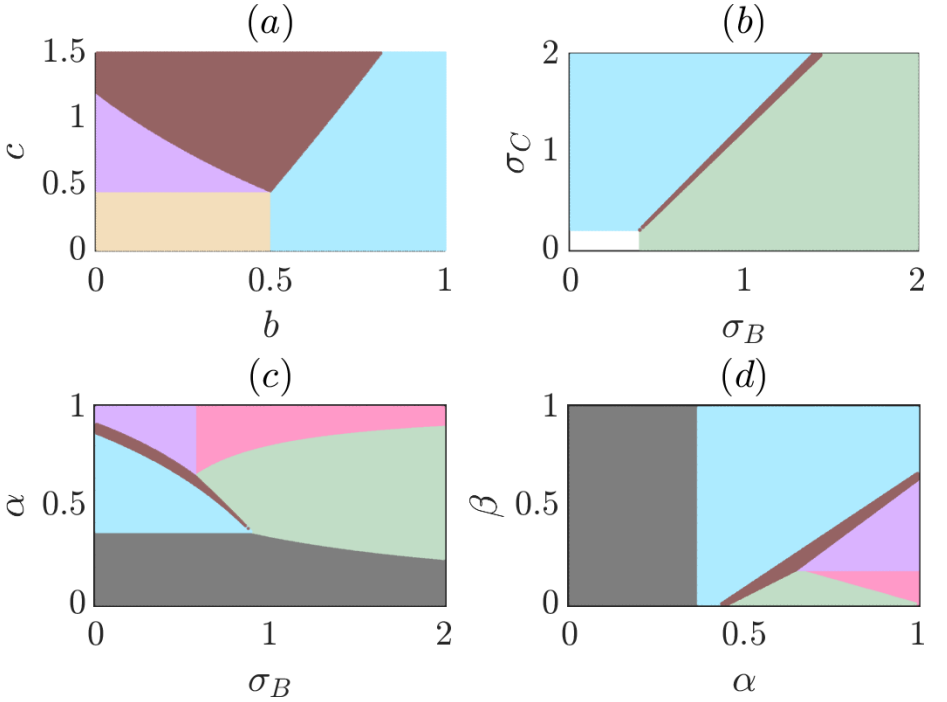

Figure 6. Transitive dominance in the payoff of strategic species delivers various stable strategic regimes over two-dimensional spans of different parameters: these figure diagrams depict two-dimensional parameter spans of our system (equation (2.4)) at $p = 0$. (*a*) Ensures the variation of two payoff attributes b and c, whereas (*b*) showcases the two-dimensional regime in variation of the free space-induced attributes σ_B and σ_C. (*c*) Deals with the span of σ_B with a extinction (*d*) depicts the consequences for varying two rates of extinction α, and β simultaneously. We set our initial abundance of species to be (0.3,0.3,0.3), considering over 50 000 times up to 60 000 time iterations. We divide the proposed ranges of the parameters by taking a step-length of $h = 0.005$. In (*a*,*b*) and (*d*), we vary two similar factors that contribute to shaping our eco-evolutionary system, whereas in (*c*), we depict the inter-dependencies of two different class factors σ_B, and α.

advantages for B-strategy species, creating a favourable environment for B-strategic traits to coexist with C-strategic ones (purple region, representing $A_5(0, y^*, z^*)$). This region gradually shrinks as b increases from 0 to 0.5, with $c > 0.45$. Further increasing c enhances strategy A's ability to thrive, leading to a regime where all three strategic species can coexist (brown region, representing $A_7(x^*, y^*, z^*)$). As the payoff b continues to increase beyond 0.5, the strategic stability of $A_7(x^*, y^*, z^*)$ shifts, transforming into $A_6(x^*, 0, z^*)$ as both payoff values rise.

As portrayed in figure 6*b*, if we look at the phase diagram owing to the simultaneous variations of two different free space raised benefits σ_B and σ_C, a *benevolent feature* is evident. A square-shaped region appears with boundaries along $\sigma_B = 0.4$ and $\sigma_C = 0.2$, in which none of the equilibrium points are stable. Moreover, this portion drives cyclic oscillations in the abundance of the strategic species instead of having a transitive form in their payoffs (unmarked portion in figure 6*b*). We discuss more of these features in the following section. Following the unstable presence of the strategic species, our transitive evolutionary model produces three stable regimes. On further increasing σ_B from 0.4, a large stable field is found, where the hierarchical capability of strategy A is seen, also providing direct evolutionary ease to the B-strategic species. Eventually, the stable planar equilibrium $A_4(x^*, y^*, 0)$ (olive-green region) appears in the elevated margin of σ_B, though its span decreases with increasing σ_C. Amplifying σ_C results in the same evolutionary sustainability for species with strategy C, alongside strategy A, forming a stable state $A_6(x^*, 0, z^*)$ for a significant portion of the parameter space (cyan region). Between

these two stable planar states, a thin region emerges, influenced by both factors σ_B and σ_C. In this scenario, B-strategic species also achieve persistence, coexisting alongside the other two strategies ($A_7(x^*, y^*, z^*)$ state denoted by the thin brown region).

Figure 6*c* shows that throughout the range of σ_B, concerning the mortality rate α of the A-species shapes several strategic stable regimes. As α is considered a key factor influencing the potential of the A strategy, regions with a shallow frequency of α up to 0.36 result in a state where only the A-strategic species can survive (grey region representing $A_1(x^*, 0,0)$). A further increment in α drives its contemporary strategies C, and then B to conquer the rule along with A, resulting in portions for the stable states $A_6(x^*, 0, z^*)$ (cyan space), and $A_7(x^*, y^*, z^*)$ (brown region) consecutively. On inducing a higher extinction factor α, strategy A loses its capability to become hierarchically dominant over the others, and a regime emerges where no A-strategic species survive, while those with strategies B and C persist (a purple portion delivering $A_5(0, y^*, z^*)$). In this high-morbidity zone for species A, a certain increase in the free-space induced factor σ_B benefits strategy B, offering a favourable window for the B-strategic species to dominate the terrain uniquely (pink region representing $A_2(0, y^*, 0)$). Also, comparatively low values of α allow our system to support a reasonable range in which both A and B-strategic traits can be sustained together (olive-green regime standing for $A_4(x^*, y^*, 0)$).

In the analysis of the range determined by two mortality factors, α and β (affecting the B-species), a sufficient portion emerges for the exclusive survival of the A-strategic species (grey region in figure 6*d*) up to $\alpha = 0.37$, and independent of β. On crossing this mark, our transitive eco-evolutionary system unveils the stable $A_6(x^*, 0, z^*)$ state, where A and C strategic traits survive simultaneously. Emergent variations in strategic stability are observed in the lower frequency regimes of β. Starting from $\alpha = 0.43$, a narrow region emerges with the simultaneous increase of the parameter values, where the coexistence of all three strategies is noted ($A_7(x^*, y^*, z^*)$ described by the brown portion). Below this coexistence belt, three consecutive strategic stabilities are observed: first, the stable concurrence of species driven by strategies A and B; second, a brief period of solo dominance by the B strategy when α reaches a very high frequency; and last, on implementing higher frequency of β a stable regime where B and C-strategic species coexist up to $\alpha = 1$ (represented by olive-green, pink and purple regions).

(c) Transitive payoff structure drives cyclic oscillations among the strategic species

A key focus of our study is the intricate transitive structure in payoff attributes, highlighting the diverse strategic distributions arising from the three proposed strategies: A, B and C. Although we have previously discussed how various species, including those with weaker strategies, can persist and maintain their populations despite the hierarchical dominance of strategy A, we now turn our attention to how this stable coexistence of these strategies eventually gives way to instability and the emergence of oscillations. *Despite the system's development being firmly rooted in a transitive framework, with no inherent guarantee that the C strategy will excel, the unstable regime nevertheless produces fully cyclic oscillations. This instability can even allow the weaker strategy to achieve the highest amplitude compared with the others* (see figure 7*a*).

We thus execute an experiment with the completely transitive payoff structure (i.e. by taking $p = 0$ in matrix (2.2)) and fixing parameter values as $a = 0.6$, $b = 0.1$, $c = 0.4$, $\sigma_B = 0.8$, $\sigma_C = 0.9$, $\alpha = 0.35$, $\beta = 0.2$ and $\gamma = 0.08$. Keeping this set fixed, we adjust the frequency of σ_A within the range [1,1.3]. With this varying span of σ_A, our transitive evolutionary system takes the following form:

$$\begin{aligned}\dot{x} &= x[-\sigma_A x + (0.6 - \sigma_A)y + (0.1 - \sigma_A)z + (\sigma_A - 0.35)],\\ \dot{y} &= y(-1.4x - 0.8y - 0.4z + 0.6),\\ \dot{z} &= z(-x - 1.3y - 0.9z + 0.82).\end{aligned} \tag{4.2}$$

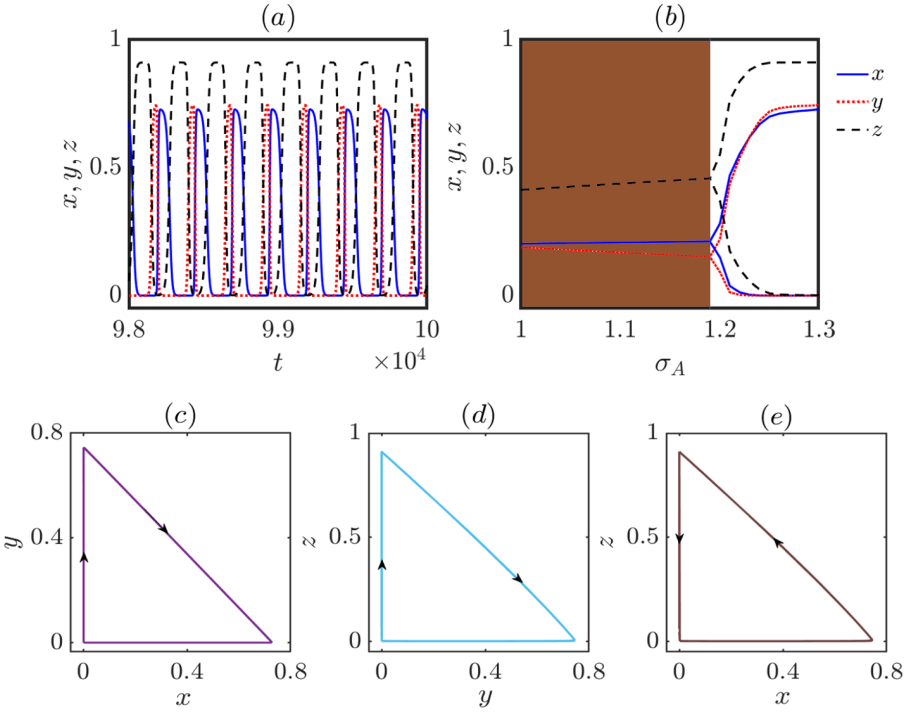

Figure 7. Cyclic oscillation in transitive payoff model (taking $p = 0$) and the route to instability concerning σ_A with the phase portrait diagrams on the cyclic oscillation: varying σ_A from 1 up to 1.3 causes a super-critical Hopf bifurcation at $\sigma_A = 1.2$, breaking the stable abundance of strategic species into oscillations (*b*). We see the oscillatory patterns of the frequency of the species in (*a*) for $\sigma_A = 1.3$, and choosing other parameters at $a = 0.6, b = 0.1, c = 0.4, \sigma_B = 0.8, \sigma_C = 0.9, \alpha = 0.35, \beta = 0.2$ and $\gamma = 0.08$. (*c*,*d*) and (*e*) show the two-dimensional phase portrait diagrams resulting in closed trajectories by the cyclic oscillation in the strategic species. We indicate the stable coexisting species' portion by brown background and the unstable regime remains uncoloured for better understanding, and we also add small arrows to navigate the directions of oscillation in (*c*–*e*) .

From the initialization of this varying span of σ_A, our system (equation (4.2)) evolves into a stable pattern where three proposed strategies with their kind species coexist in the same habitat (brown region in figure 7*b*). Naturally, the trajectory of species takes an obvious direction: as the frequency of σ_A increases, the abundance of A-strategic species rises monotonically. Conversely, with a significant decrease in a to 0.6, the chances for the survivability of the B-species declines correspondingly. Interestingly, the C-strategic species, which experience only a minor reduction from interactions with A-strategic species (with $b = 0.1$), manage to gradually increase their abundance. This growth is supported by the progressive decline in the effectiveness of strategy B. On the other hand, the overall frequency of the C-strategic species remains significantly higher than that of the other strategies. The C-strategic species face a comparatively lower risk of extinction ($\gamma = 0.08 < \alpha$, and β) throughout this period of steady coexistence, despite the A species having a notably higher replication advantage from the free space. Considering the mathematical analysis for this stable state $A_7(x^*, y^*, z^*)$, an increase in the parameter value up to $\sigma_A = 1.2$ reveals a consistently negative real part in the complex conjugate eigenvalues. This observation supports our claim of the stable coexistence of the species. Upon reaching $\sigma_A = 1.2$, the system analysis fails to deliver a stable frequency of the traits. Moreover, the eigenvalues we find for $A_7(0.2118, 0.1492, 0.4603)$ at $\sigma_A = 1.2$ are -0.7878, and $\pm 0.1250i$, which aligns well with the analysis indicating the occurrence of a super-critical Hopf bifurcation as σ_A increases. For values of σ_A greater than 1.2 (uncoloured region in figure 7*b*), the complex eigenvalues hold a form of $w_1 + iw_2$, where $w_1 > 0$ throughout the unstable

portion, suggesting instability for interior fixed point $A_7(x^*, y^*, z^*)$ of the system (equation (4.2)). Nevertheless, none of the other stationary points within the strategic framework yield a stable regime. This unstable environment transitions into oscillations, similar to those observed in the study of a fully cyclic structured payoff. We thus set $\sigma_A = 1.3$ to examine the nature of oscillations within these unstable equilibrium regimes. For $\sigma_A = 1.3$, our system can produce fixed points as $A_0(0,0,0)$, $A_1(0.7308,0,0)$, $A_2(0,0.75,0)$, $A_3(0,0,0.911)$ and $A_7(0.2159,0.1317,0.481)$; each of them prove to be unstable (see appendix A). The planar stationary points fail to exist for the chosen parameter set owing to their negative frequency, which we discuss in the appendix A. However, the oscillations exhibit characteristics of pseudo-stable regimes when strategy A's species begin to dominate the entire habitat (blue solid line in figure 7*a*), the abundance of the other kinds remain low. Interestingly, the weakest strategy C according to the theory of transitive dominance is seen to invade strategy A and overpower the entire terrain achieving a remarkable increase in habitat occupation, reaching up to 91% (black dashed line in figure 7*a*). With sufficient time for the weaker C strategy and its associated species, the eco-evolutionary environment eventually sees strategy B overpowering C, resulting in a significant increase where B occupies nearly 75% of the habitat. Subsequently, strategy B struggles against strategy A, leading to periodic dominance of A-strategic species in the habitat. *This creates a cyclic pattern of oscillation among the three strategies A, B and C, regulating their respective populations, despite the fully transitive structured payoff values*.

5. Discussion and conclusion

The transitive pattern dominance in eco-evolutionary dynamics unveils a complex interplay of species with strategies, where hierarchical relationships drive evolutionary outcomes [40]. Unlike purely cyclic systems, where species follow a predictable loop of victories and defeats, this transitive nature introduces a directional flow of dominance that shapes the ecological structure [41]. Ultimately, this transitive dominance establishes a dynamic yet orderly framework that regulates species abundance, interactions and long-term survival within ecological systems. The transition from transitive dominance to cyclic dominance is a dynamic process influenced by environmental interactions and evolutionary pressures. The hierarchical order that if species A dominates species B and species B dominates species C, species A will also dominate species C creates a strict, linear structure of dominance. However, in complex ecological systems, the introduction of frequency-dependent selection, spatial heterogeneity and resource competition can disrupt this linearity, leading to cyclic dominance. Cyclic dominance occurs when species form a non-hierarchical relationship, as seen in the rock-paper-scissors dynamics, where each species can dominate one but be dominated by the other. This cyclical interaction is advantageous in maintaining biodiversity, as no single species can outcompete others, thus preventing competitive exclusion. Studies in microbial communities (e.g. *Escherichia coli*) and predator–prey dynamics have shown how environmental pressures, such as fluctuating resources or spatial constraints, can shift dominance hierarchies towards cyclic patterns. The cyclical nature of these interactions ensures coexistence and stabilizes ecosystems by continuously recycling competitive advantages among species. Ecological models suggest that systems exhibiting such dynamics tend to be more resilient to disturbances, with species continually adapting to the pressures imposed by others, preventing monopolization and supporting overall ecosystem health.

Through this article, we have presented a thorough analysis of the mechanisms that facilitate the transition from transitive dominance to cyclic dominance in ecological communities, utilizing the concepts of evolutionary game theory. By employing a multigame framework and integrating appropriate models, we have identified crucial factors and approaches that drive these transitions. We have specifically designed the multigame model so that the games characterizing transitive dominance and cyclic dominance are played with complementary

probabilities. We have presented comprehensive numerical simulations and an analytical approach for our mathematical model, focused on the stability of various equilibrium points. Our study emphasizes that the transition from a linear hierarchy to a cyclical structure is influenced not only by factors independent of the game but also by intrinsic game parameters and ecological variables. To be precise, the probability of selecting different games influences the shift from a transitive to a cyclical arrangement of evolutionary strategies. In addition, our research reveals that the benefits provided by free space can play a major role in promoting the transition from a linear to a cyclical dominance pattern. Our findings thus contribute to the growing body of knowledge on eco-evolutionary dynamics and highlight the need to account for multigame dynamics and various ecological factors when modelling natural ecosystems.

Although our multi-game framework offers valuable insight into the transition between transitive and cyclic dominance, it also involves certain limitations. One key constraint lies in the assumption of ecological free space, which is treated as a uniform and constant resource. In reality, free space availability may vary spatially and temporally, influencing species interactions in more complex ways than the model accounts for. A promising direction for future research though includes exploration of how higher-order interactions, such as triadic or multi-species dependencies, influence the transition between transitive and cyclic dominance. Investigating the role of temporal environmental fluctuations, adaptive strategies and spatial network structures in shaping these dominance patterns could provide deeper insights. In addition, extending the multigame framework to incorporate co-evolutionary feedback and real-world ecological data would enhance its applicability and predictive power for complex ecosystems.

Data accessibility. The codes used in the simulations for this article is available openly on the GitHub repository: https://github.com/me-souravpamu/transitive.git.

Declaration of AI use. We have not used AI-assisted technologies in creating this article.

Authors' contributions. S.R.: conceptualization, data curation, formal analysis, investigation, methodology, resources, software, visualization, writing—original draft; S.M.: conceptualization, data curation, formal analysis, investigation, methodology, resources, software, validation, writing—original draft; M.P.: conceptualization, project administration, supervision, visualization, writing—review and editing; D.G.: conceptualization, project administration, supervision, validation, visualization, writing—review and editing

All authors gave final approval for publication and agreed to be held accountable for the work performed therein.

Conflict of interest declaration. We declare we have no competing interests.

Funding. S.R was supported by the University Grants Commission (Ref no: 201610073701). M.P.was supported by the Slovenian Research and Innovation Agency (Javna agencija za znanstvenoraziskovalno in inovacijsko dejavnost Republike Slovenije) (Grant Nos. P1-0403 and N1-0232).

Appendix A

We execute linear stability analysis of our mathematical framework (equation (2.4)) formed as a passage to overcome the hierarchical nature of the stronger ability (here A strategy and x becoming its frequency) through the transitive dominance tuning its pattern to dominate as one of the abilities to becoming fully cyclic. In this section, we capture the complete linear stability analysis by calculating the Jacobian of the system (equation (2.4)) about any fixed point $A(x^*, y^*, z^*)$ as

$$J = \begin{bmatrix} k_{11} & k_{12} & k_{13} \\ k_{21} & k_{22} & k_{23} \\ k_{31} & k_{32} & k_{33} \end{bmatrix}, \tag{A 1}$$

where $k_{11} = -2\sigma_A x^* + (a - \sigma_A)y^* + (b - 2pb - \sigma_A)z^* + (\sigma_A - \alpha)$,
$k_{12} = (a - \sigma_A)x^*$, $k_{13} = (b - 2pb - \sigma_A)x^*$,

$k_{21} = -(a + \sigma_A)y^*$,
$k_{22} = -(a + \sigma_B)x^* - 2\sigma_B y^* + (c - \sigma_B)z^* + (\sigma_B - \beta)$,
$k_{23} = (c - \sigma_B)y^*$, $k_{31} = (2pb - b - \sigma_C)z^*$,
$k_{32} = -(c + \sigma_C)z^*$, and
$k_{33} = (2pb - b - \sigma_C)x^* - (c + \sigma_C)y^* - 2\sigma_C z^* + (\sigma_C - \gamma)$.

The characteristic equation of the Jacobian matrix J (equation (A 1)) with respect to the arbitrary equilibrium point $A(x^*, y^*, z^*)$ can emerge:
$\lambda^3 - \kappa_1\lambda^2 + \kappa_2\lambda - \kappa_3 = 0$, where λ's are the solution of the characteristic equation and produce three eigenvalues depending on the parameter values induced to the system. Here,
$\kappa_1 = Trace(J) = k_{11} + k_{22} + k_{33}$,
$\kappa_2 = K_{11} + K_{22} + K_{33} = k_{11}k_{22} + k_{22}k_{33} + k_{33}k_{11} - k_{12}k_{21} - k_{13}k_{31} - k_{23}k_{32}$, and
$\kappa_3 = Det(J) = -(k_{11}k_{23}k_{32} + k_{22}k_{31}k_{13} + k_{33}k_{12}k_{21} - k_{11}k_{22}k_{33} - k_{12}k_{23}k_{31} - k_{13}k_{32}k_{21})$.
Thus the equilibrium $A(x^*, y^*, z^*)$ is asymptotically stable if

- $Trace(J) = \kappa_1 < 0$, i.e., $k_{11} + k_{22} + k_{33} < 0$,
- $K_{11} + K_{22} + K_{33} > 0$, i.e. $k_{11}k_{22} + k_{22}k_{33} + k_{33}k_{11} > k_{12}k_{21} + k_{13}k_{31} + k_{23}k_{32}$,
- $Det(J) = \kappa_3 < 0$, i.e., $k_{11}k_{23}k_{32} + k_{22}k_{31}k_{13} + k_{33}k_{12}k_{21} > k_{11}k_{22}k_{33} + k_{12}k_{23}k_{31} + k_{13}k_{32}k_{21}$, and
- $Trace(J)(K_{11} + K_{22} + K_{33}) < Det(J)$, i.e.
  $(k_{11} + k_{22} + k_{33})(k_{11}k_{22} + k_{22}k_{33} + k_{33}k_{11} - k_{12}k_{21} - k_{13}k_{31} - k_{23}k_{32}) + (k_{11}k_{23}k_{32} + k_{22}k_{31}k_{13}.$
  $+ k_{33}k_{12}k_{21} - k_{11}k_{22}k_{33} - k_{12}k_{23}k_{31} - k_{13}k_{32}k_{21}) < 0$

Our mathematical eco-evolutionary framework (equation (2.4)) produces eight equilibrium points to observe eight different strategic distributions of three proposed strategies A, B and C.

A.1. Strategic equilibriums of the system

A.1.1. The null equilibrium

This equilibrium appears when all state variables become zero. Being a trivial fixed point of our model (equation (2.4)), $A_0(0,0,0)$ is stable, only when $\sigma_A < \alpha$, $\sigma_B < \beta$ and $\sigma_C < \gamma$, suggesting that the stability of $A_0(0,0,0)$ holds only when the respective death rates of the strategic species exceed their free space-induced attributes. Biologically, this null attractor refers to an environment that consists of no species in it.

A.1.2. Axial fixed points

In the analysis of our eco-evolutionary system (equation (2.4)), the axial fixed points, or axial attractors, represent ecological scenarios where a single strategy and its associated species dominate, ensuring their persistence in the evolutionary race. Notably, we identify three distinct axial attractors, each independent of specific payoff attributes but governed by the availability of ecological niches or resource-free spaces, characterized by the positive signatures σ_A, σ_B and σ_C. These signatures reflect the intrinsic capacity of each strategy to monopolize ecological space, emphasizing their role in shaping competitive exclusion and species coexistence:

- $A_1(x^*, 0, 0)$, the first axial attractor, where only the A-strategic species persist in the environment and reflect a hierarchical dominance order that ensures a transitive payoff structure among the three competing strategies in our model; here $x^* = 1 - \frac{\alpha}{\sigma_A}$ and $A_1(1 - \frac{\alpha}{\sigma_A}, 0, 0)$ is stable when (i) $\sigma_A > \alpha$, (ii) $a(\sigma_A - \alpha) > \alpha\sigma_B - \sigma_A\beta$ and (iii) $(2pb - b)(\sigma_A - \alpha) + \alpha\sigma_C < \sigma_A\gamma$.
- $A_2(0, y^*, 0)$, the second axial fixed point, where only the B-strategic species persist in the environment, highlights a shift in dominance within the multi-game framework. As the parameter p transitions from 0 to 1, the hierarchical dominance of strategy B by strategy A progressively diminishes, reflecting a dynamic adjustment in competitive pressure.

Upon satisfying the conditions outlined below, this attractor stabilizes, signifying a steady state where strategy B monopolizes the ecological niche, potentially influencing the evolutionary landscape by suppressing competing strategies. Here, $y^* = 1 - \frac{\beta}{\sigma_B}$ and $A_2(0, \frac{\beta}{\sigma_B}, 0)$ is stable under the conditions, (i) $\sigma_B > \beta$, (ii) $\sigma_B(a-\alpha) + \beta(\sigma_A - a) < 0$ and (iii) $\beta(c + \sigma_C) < \sigma_B(c + \gamma)$.

— $A_3(0,0,z^*)$, the third axial attractor grants the C-strategic species the highest potential to dominate the entire habitat, even within a constrained regime where payoffs exert bilateral pressure on strategy C from both strategies A and B. Despite this dual challenge in the transitive regime of the strategic payoffs, the attractor underscores the resilience and competitive edge of strategy C, enabling it to outlast its rivals and maintain ecological dominance under specific evolutionary conditions. Here, $z^* = 1 - \frac{\gamma}{\sigma_C}$ and $A_3(0,0,1 - \frac{\gamma}{\sigma_C})$ is stable when (i) $\sigma_C > \gamma$, (ii) $(b - 2pb - \sigma_A)(\sigma_C - \gamma) + \sigma_C(\sigma_A - \alpha) < 0$ and (iii) $(c - \sigma_B)(\sigma_C - \gamma) + \sigma_C(\sigma_B - \beta) < 0$.

We note that these axial attractors do not depend on any payoff amounts, rather only the free space produced, non-zero attributes that let these attractors enable.

A.1.3. Planar fixed point

The planar fixed points derived from our model (equation (2.4)) delineate dual-strategy regimes, where only two of the three strategies—A, B or C—coexist and sustain their presence in the evolutionary race. These equilibria capture the competitive balance between the surviving strategies, highlighting their mutual dependence and the exclusion of the third, ultimately shaping the dynamics of partial coexistence within the ecological system. The three planar attractors of the system (equation (2.4)) are described below.

— $A_4(x^*, y^*, 0)$, the first planar fixed point represents a coexistence state where only the A and B species persist, jointly out-competing and eliminating the weakest transitive species, C. This equilibrium highlights the hierarchical dominance of strategies A and B, where their combined competitive strength prevents C from sustaining in the evolutionary race.

Here, $x^* = -\frac{a\beta - a\sigma_B + \alpha\sigma_B - \beta\sigma_A}{a\sigma_B - a\sigma_A + a^2}$, and $y^* = \frac{a\alpha - a\sigma_A + \alpha\sigma_B - \beta\sigma_A}{a\sigma_B - a\sigma_A + a^2}$.
So, $A_4(-\frac{a\beta - a\sigma_B + \alpha\sigma_B - \beta\sigma_A}{a\sigma_B - a\sigma_A + a^2}, \frac{a\alpha - a\sigma_A + \alpha\sigma_B - \beta\sigma_A}{a\sigma_B - a\sigma_A + a^2}, 0)$ is the planar fixed point of our system.

— $A_5(0, y^*, z^*)$, the second planar attractor, one of the most ecologically significant state, represents coexistence in which the transitive weaker strategies B and C coexist, overcoming and eliminating the hierarchically dominant strategy A. This attractor underscores the potential for collaborative survival of subordinate strategies, highlighting how ecological interactions and environmental conditions can reverse hierarchical dominance and sustain biodiversity.

In this attractor, $y^* = -\frac{\beta\sigma_C - c\sigma_C + c\gamma - \sigma_B\gamma}{c\sigma_C - c\sigma_B + c^2}$, and $z^* = \frac{\beta c + \beta\sigma_C - c\sigma_B - \sigma_B\gamma}{c\sigma_C - c\sigma_B + c^2}$.
So, $A_5(0, -\frac{\beta\sigma_C - c\sigma_C + c\gamma - \sigma_B\gamma}{c\sigma_C - c\sigma_B + c^2}, \frac{\beta c + \beta\sigma_C - c\sigma_B - \sigma_B\gamma}{c\sigma_C - c\sigma_B + c^2})$ is another planar stationary point of our system.

— $A_6(x^*, 0, z^*)$, the third planar attractor represents a coexistence state where the hierarchically strongest strategy A and the weakest strategy C persist simultaneously. This attractor illustrates a counterintuitive dynamic, where the extreme ends of the domi-

nance hierarchy stabilize together, potentially driven by indirect interactions or ecological constraints that prevent intermediate strategy B from surviving. Here

$$x^* = -\frac{\alpha\sigma_C - b\sigma_C + b\gamma - \sigma_A\gamma + 2bp\sigma_C - 2bp\gamma}{b\sigma_C - b\sigma_A - 4b^2p + b^2 + 4b^2p^2 + 2bp\sigma_A - 2bp\sigma_C}, \text{ and}$$

$$z^* = \frac{\alpha b + \alpha\sigma_C - b\sigma_A - \sigma_A\gamma - 2\alpha bp + 2bp\sigma_A}{b\sigma_C - b\sigma_A - 4b^2p + b^2 + 4b^2p^2 + 2bp\sigma_A - 2bp\sigma_C}.$$

Thus, $A_6(-\frac{\alpha\sigma_C - b\sigma_C + b\gamma - \sigma_A\gamma + 2bp\sigma_C - 2bp\gamma}{b\sigma_C - b\sigma_A - 4b^2p + b^2 + 4b^2p^2 + 2bp\sigma_A - 2bp\sigma_C}, 0, \frac{\alpha b + \alpha\sigma_C - b\sigma_A - \sigma_A\gamma - 2\alpha bp + 2bp\sigma_A}{b\sigma_C - b\sigma_A - 4b^2p + b^2 + 4b^2p^2 + 2bp\sigma_A - 2bp\sigma_C})$ is the last planar stationary point of our system.

A.1.4.The non-trivial coexisting fixed point

The coexistence state of the three simultaneous strategies A, B and C represents the most evolutionarily significant equilibrium in eco-evolutionary theory, as it embodies a dynamic balance where no single strategy dominates. This state promotes long-term biodiversity, stabilizes ecological interactions, and reflects the complex interplay of competition, cooperation and adaptation necessary for ecosystem resilience.

We represent this attractor as $A_7(x^*, y^*, z^*)$, where

$x^* = -\frac{\Delta_1}{\Delta}, y^* = -\frac{\Delta_2}{\Delta}, z^* = \frac{\Delta_3}{\Delta}$,

and

where $\Delta = a^2\sigma_C + b^2\sigma_B + c^2\sigma_A - 4b^2p\sigma_B + 4b^2p^2\sigma_B - ab\sigma_B - ab\sigma_C + ac\sigma_A + ac\sigma_C - bc\sigma_A - bc\sigma_B + 2abp\sigma_B + 2abp\sigma_C + 2bcp\sigma_A + 2bcp\sigma_B$,

$\Delta_1 = \alpha c^2 - c^2\sigma_A - b\beta c + a\beta\sigma_C - ac\sigma_C - b\beta\sigma_C - \alpha c\sigma_B + \alpha c\sigma_C + bc\sigma_B + \beta c\sigma_A + ac\gamma - a\sigma_B\gamma + b\sigma_B\gamma - c\sigma_A\gamma + 2b\beta p\sigma_C - 2bcp\sigma_B - 2bp\sigma_B\gamma + 2b\beta cp$,

$\Delta_2 = b^2\beta - b^2\sigma_B + 4b^2p\sigma_B + 4b^2\beta p^2 - 4b^2p^2\sigma_B - \alpha bc - a\alpha\sigma_C + ab\sigma_C + \alpha b\sigma_B - b\beta\sigma_A + b\beta\sigma_C - \alpha c\sigma_C + bc\sigma_A - ab\gamma + a\sigma_A\gamma - b\sigma_B\gamma + c\sigma_A\gamma - 4b^2\beta p - 2abp\sigma_C - 2\alpha bp\sigma_B + 2b\beta p\sigma_A - 2b\beta p\sigma_C - 2bcp\sigma_A + 2ab p\gamma + 2bp\sigma_B\gamma + 2\alpha bcp$, and

$\Delta_3 = a^2\sigma_C - a^2\gamma + ab\beta - a\alpha c - a\alpha\sigma_C - ab\sigma_B + a\beta\sigma_C + \alpha b\sigma_B + ac\sigma_A - b\beta\sigma_A - \alpha c\sigma_B + \beta c\sigma_A + a\sigma_A\gamma - a\sigma_B\gamma + 2abp\sigma_B - 2\alpha bp\sigma_B + 2b\beta p\sigma_A - 2ab\beta p$.

References

1. Pelletier F, Garant D, Hendry AP. 2009 Eco-evolutionary dynamics. *Philos. Trans. R. Soc. B* **364**, 1483–1489. (doi:10.1098/rstb.2009.0027)
2. Hendry AP. 2016 Population Dynamics. In *Eco-evolutionary dynamics*. Princeton University Press. (doi:10.23943/princeton/9780691145433.003.0007)
3. Nowak MA. 2006 *Evolutionary Dynamics: Exploring the Equations of Life*. Harvard University Press.
4. Nowak MA, May RM. 1992 Evolutionary games and spatial *chaos*. *Nature* **359**, 826–829. (doi:10.1038/359826a0)
5. Hofbauer J, Sigmund K *et al*. 1998 *Evolutionary Games and Population Dynamics*. Cambridge University Press. (doi:10.1017/CBO9781139173179). See https://www.cambridge.org/core/product/identifier/9781139173179/type/book.
6. Szabó G, Fath G. 2007 Evolutionary Games on Graphs. *Phys. Rep.* **446**, 97–216.
7. Perc M, Gómez-Gardeñes J, Szolnoki A, Floría LM, Moreno Y. 2013 Evolutionary dynamics of group interactions on structured populations: a review. *J. R. Soc. Interface* **10**, 20120997. (doi:10.1098/rsif.2012.0997)
8. Wang Z, Wang L, Szolnoki A, Perc M. 2015 Evolutionary games on multilayer networks: a colloquium. *Eur. Phys. J. B* **88**. (doi:10.1140/epjb/e2015-60270-7)

9. Aleta A, Moreno Y. 2019 The dynamics of collective social behavior in a crowd controlled game. *EPJ Data Sci.* **8**, 22. (doi:10.1140/epjds/s13688-019-0200-1)
10. Gómez-Gardeñes J, Gracia-Lázaro C, Floría LM, Moreno Y. 2012 Evolutionary dynamics on interdependent populations. *Phys. Rev. E* **86**, 056113. (doi:10.1103/physreve.86.056113)
11. Wang X, Fu F. 2020 Eco-evolutionary dynamics with environmental feedback: Cooperation in a changing world. *Europhys. Lett.* **132**, 10001. (doi:10.1209/0295-5075/132/10001)
12. Fussmann GF, Loreau M, Abrams PA. 2007 Eco-evolutionary dynamics of communities and ecosystems. *Funct. Ecol.* **21**, 465–477. (doi:10.1111/j.1365-2435.2007.01275.x)
13. Tilman D. 1994 Competition and Biodiversity in Spatially Structured Habitats. *Ecology* **75**, 2–16. (doi:10.2307/1939377)
14. Beacham J. 2003 Models of Dominance Hierarchy Formation: Effects of Prior Experience and Intrinsic Traits. *Behaviour* **140**, 1275–1303. (doi:10.1163/156853903771980594)
15. Plowes NJR. 2008 Self Organized Conflicts in Territorial Ants. University of Connecticut.
16. McGlynn TP. 2006 Ants on the Move: Resource Limitation of a Litter-nesting Ant Community in Costa Rica [1]. *Biotropica* **38**, 419–427. (doi:10.1111/j.1744-7429.2006.00153.x)
17. Gibson R, Barnes M, Atkinson R. 2001 Territorialdamselfishesasdeterminantsofthestructure of benthic communities on coral reefs. *Oceanogr. Mar. Biol. Annu. Rev.* **39**, 355–389. (doi:10.1007/s003380000087)
18. Sade DS. 1973 Determinance of Dominance in a group of Free Ranging Rhesus Monkeys. In *Social communication among primates*, pp. 99–113, vol. **14**. (doi:10.1007/BF01731357)
19. Szolnoki A, Mobilia M, Jiang LL, Szczesny B, Rucklidge AM, Perc M. 2014 Cyclic dominance in evolutionary games: a review. *J. R. Soc. Interface* **11**, 20140735. (doi:10.1098/rsif.2014.0735)
20. Artiges E, Gracia-Lázaro C, Floría LM, Moreno Y. 2019 Replicator population dynamics of group interactions: Broken symmetry, thresholds for metastability, and macroscopic behavior. *Phys. Rev. E* **100**, 052307. (doi:10.1103/physreve.100.052307)
21. Szolnoki A, Vukov J, Perc M. 2014 From pairwise to group interactions in games of cyclic dominance. *Phys. Rev. E* **89**, 062125. (doi:10.1103/physreve.89.062125)
22. Szolnoki A, Perc M. 2016 Biodiversity in models of cyclic dominance is preserved by heterogeneity in site-specific invasion rates. *Sci. Rep.* **6**, 38608. (doi:10.1038/srep38608)
23. Guo H, Song Z, Geček S, Li X, Jusup M, Perc M, Moreno Y, Boccaletti S, Wang Z. 2020 A novel route to cyclic dominance in voluntary social dilemmas. *J. R. Soc. Interface* **17**, 20190789. (doi:10.1098/rsif.2019.0789)
24. Nag Chowdhury S, Kundu S, Banerjee J, Perc M, Ghosh D. 2021 Eco-evolutionary dynamics of cooperation in the presence of policing. *J. Theor. Biol.* **518**, 110606. (doi:10.1016/j.jtbi.2021.110606)
25. Nag Chowdhury S, Banerjee J, Perc M, Ghosh D. 2023 Eco-evolutionary cyclic dominance among predators, prey, and parasites. *J. Theor. Biol.* **564**, 111446. (doi:10.1016/j.jtbi.2023.111446)
26. Chowdhury SN, Kundu S, Perc M, Ghosh D. 2021 Complex evolutionary dynamics due to punishment and free space in ecological multigames. *Proc. R. Soc. A* **477**, 20210397. (doi:10.1098/rspa.2021.0397)
27. Roy S, Nag Chowdhury S, Mali PC, Perc M, Ghosh D. 2022 Eco-evolutionary dynamics of multigames with mutations. *PLoS One* **17**, e0272719. (doi:10.1371/journal.pone.0272719)
28. Szolnoki A, Perc M. 2014 Coevolutionary success-driven multigames. *Europhys. Lett.* **108**, 28004. (doi:10.1209/0295-5075/108/28004)
29. Perc M, Szolnoki A. 2010 Coevolutionary games—A *mini* review. *Biosystems* **99**, 109–125. (doi:10.1016/j.biosystems.2009.10.003)
30. Roy S, Nag Chowdhury S, Kundu S, Sar GK, Banerjee J, Rakshit B, Mali PC, Perc M, Ghosh D. 2023 Time delays shape the eco-evolutionary dynamics of cooperation. *Sci. Rep.* **13**, 3. (doi:10.1038/s41598-023-41519-1)
31. Majhi S. 2023 Cooperation driven by alike interactions in presence of social viscosity. *Chaos* **33**, 073117. (doi:10.1063/5.0153650)
32. Wang Z, Szolnoki A, Perc M. 2014 Different perceptions of social dilemmas: Evolutionary multigames in structured populations. *Phys. Rev. E* **90**, 032813. (doi:10.1103/physreve.90.032813)
33. Qin J, Chen Y, Kang Y, Perc M. 2017 Social diversity promotes cooperation in spatial multigames. *Europhys. Lett.* **118**, 18002. (doi:10.1209/0295-5075/118/18002)

34. Roy S, Ghosh S, Saha A, Chandra Mali P, Perc M, Ghosh D. 2024 The eco-evolutionary dynamics of strategic species. *Proc. R. Soc. A* **480**, 20240127. (doi:10.1098/rspa.2024.0127)
35. Perc M, Jordan JJ, Rand DG, Wang Z, Boccaletti S, Szolnoki A. 2017 Statistical physics of human cooperation. *Phys. Rep.* **687**, 1–51. (doi:10.1016/j.physrep.2017.05.004)
36. Park HJ, Pichugin Y, Traulsen A. 2020 Why is cyclic dominance so rare? *eLife* **9**, e57857. (doi:10.7554/elife.57857)
37. Szolnoki A, Wang Z, Wang J, Zhu X. 2010 Dynamically generated cyclic dominance in spatial prisoner's dilemma games. *Phys. Rev. E* **82**, 036110. (doi:10.1103/physreve.82.036110)
38. Szabó G, Bodó KS, Samani KA. 2017 Separation of cyclic and starlike hierarchical dominance in evolutionary matrix games. *Phys. Rev. E* **95**, 012320. (doi:10.1103/physreve.95.012320)
39. Chatterjee S, Nag Chowdhury S, Ghosh D, Hens C. 2023 Erratum: 'Controlling species densities in structurally perturbed intransitive cycles with higher-order interactions'. *Chaos* **33**, 103122. (doi:10.1063/5.0150932)
40. Cerda X, Retana J, Cros S. 1997 Thermal Disruption of Transitive Hierarchies in Mediterranean Ant Communities. *J. Anim. Ecol.* **66**, 363. (doi:10.2307/5982)
41. McDonald DB, Shizuka D. 2013 Comparative transitive and temporal orderliness in dominance networks. *Behav. Ecol.* **24**, 511–520. (doi:10.1093/beheco/ars192)